VOICE COIL
THE PERIODICAL FOR THE LOUDSPEAKER INDUSTRY

Article prepared for www.audioXpress.com

Inductance et al. – A Closer Look at AC, Part 1

By Steve Mowry

The DC electromagnetic nonlinear mechanisms within electrodynamic audio transducer motor assemblies are fairly widely understood; however, the nonlinear AC mechanisms are typically ignored during the simulation and design phase of new transducer development. The inductance is a result of the voice coil's linkage to the AC magnetic flux. It is the behavior of this time-dependent AC flux within the motor assembly that is the focus of this article.

I will update my nonlinear model and present new information on S.M. Audio Engineering's voice-coil-emulating command files. Extensive use of graphic solution contour plots, plotted command file data output together with the equivalent circuit model are intended to shed new light on this classic electromagnetic field's topic. In the process, I discuss the new and important topics of dynamic permeability and skin effect. I will show that the inductance and inductance-related phenomena are significant sources of nonlinear behavior from within the motor assembly.

The SI unit of inductance is the "henry" (H). The equivalent electromagnetic, electric, and electromechanical units are respectively contained in equation 1.

$$(\mathrm{H}) = \left(\frac{\mathrm{V_S}}{\mathrm{A}}\right) = \left(\frac{\mathrm{Wb}}{\mathrm{A}}\right) = \left(\frac{\mathrm{Nm}}{\mathrm{A}^2}\right) \qquad (1)$$

If the rate of change of current in a circuit is 1A per second and the resulting electromotive force is 1V, then the inductance of the circuit is 1H. The henry is named after Joseph Henry (1797-1878), a Scottish-American scientist. During his lifetime, he was considered one of the greatest American scientists since Benjamin Franklin. While building electromagnets, he discovered the electromagnetic phenomenon of self-inductance.

The following discussion is from a technical engineering paper, *Nonlinear Quasi-dynamic DC and AC FEM for Electro-dynamic Audio Transducer Motor Assembly Simulation,* prepared as documentation for a PC OPERA 2d training seminar that I conducted on August 30, 2006, at Advanced Sound Products, in Malaysia. I have attempted to present the concepts in as friendly a format as possible.

MOTOR ASSEMBLY MODEL

I will present an equivalent circuit to illustrate the voice coil within the motor assembly in ***Fig. 1***.

MODEL VARIABLES:

B*l* is the DC force factor (Tm).
Bl is the AC force factor (Tm).
φ is the rate of change of the time varying AC flux (Wb/s).
r is the radius (m).
l is the length of the voice coil wire (m).
μ is the magnetic permeability (H/m).
σ is the electrical conductivity of the material (1/Ωm).
J is the eddy current density (A/m^2).
E is the electric field (V/m).
v is the input voltage from the power amplifier (V).
i is the current in the voice coil (A).
Re is the DC resistance of the voice coil (Ω).

FIGURE 1: Equivalent circuit for nonlinear DC and AC model.

R_{FM} is the resistance related to the eddy current losses within the steel (Ω).

R_{SR} is the resistance related to the eddy current losses within the shorting ring (Ω).

Le is the total self inductance of the voice coil (H).

S_{FM} is the cross-section of the steel (m^2).

x is the position of the voice coil (m).

is the velocity of the voice coil (m/s).

dx is the voice coil wind height (m).

zm is the lumped equivalent mechanical impedance (Ω) related to moving mass Mms, nonlinear termination stiffness Kms(x), and termination losses Rms.

δ is the skin depth of the "AC skin effect" (m).

The skin effect as it affects eddy current is essential to understanding inductance and the other AC effects. The skin depth δ for a sinusoidal signal is defined in equation 2.

$$\delta(i) = \frac{1}{\sqrt{\pi f \sigma \mu(i)}} (m) \qquad (2)$$

where *f* (Hz) is the frequency of the AC current, *i*. I will show that the skin depth has a nonlinear current dependence related to the dynamic permeability.

In ***Fig. 1***, the segment on the left, the AC harmonic model, is attached to ground and thus it does not change position. However, the large right-hand segment represents the moving voice coil within the magnetic gap and does change position, *x*. There are no physical wires and/or connections from the left segment to the right-hand segment. Nor are there any mechanical terminations. There are two magnetic fields interacting with the voice coil, the primary DC, and the secondary

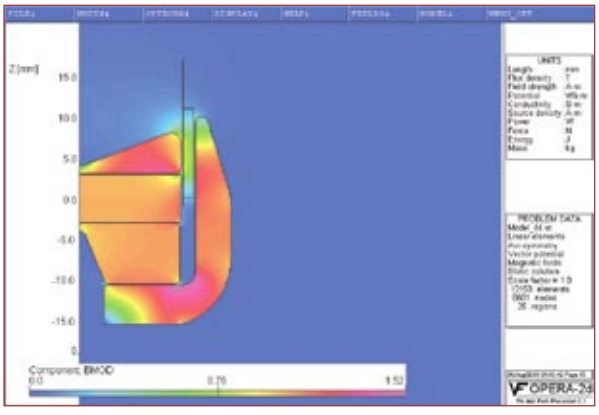

FIGURE 2: Contour plot of |B|, the magnitude of the DC flux density.

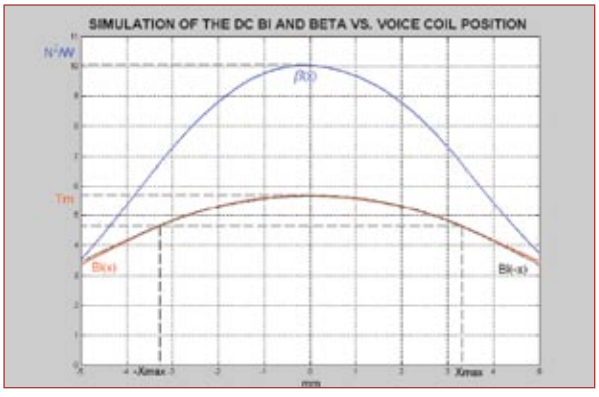

FIGURE 3: Plot of quasi-dynamic simulation of Bl(x) and β(x).

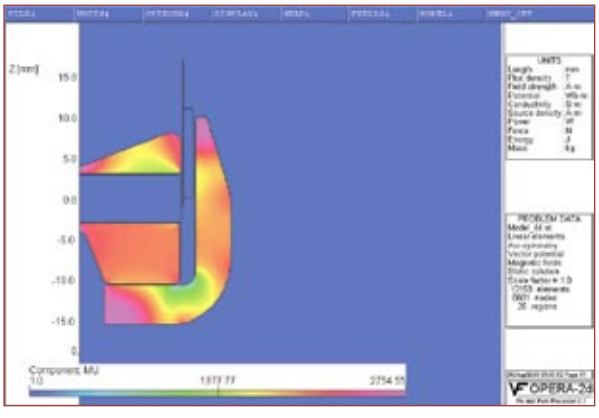

FIGURE 4: Contour plot of the relative DC permeability, μrel.

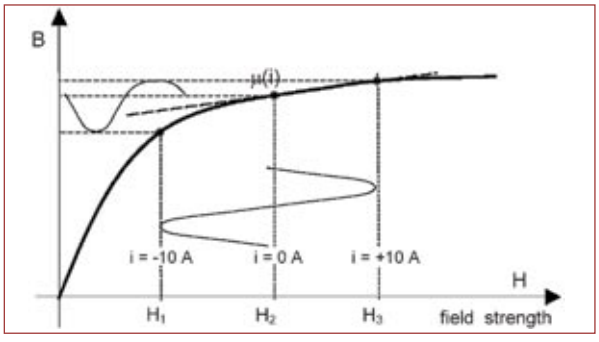

FIGURE 5: Illustration of the nonlinear dynamic permeability of steel, μ(i).

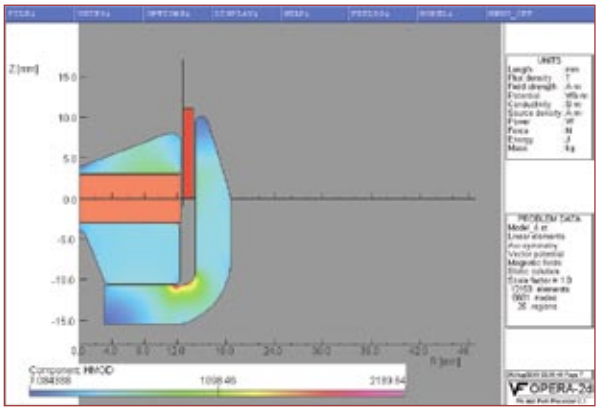

FIGURE 6: Contour plot of the DC Field strength |H| within the steel only.

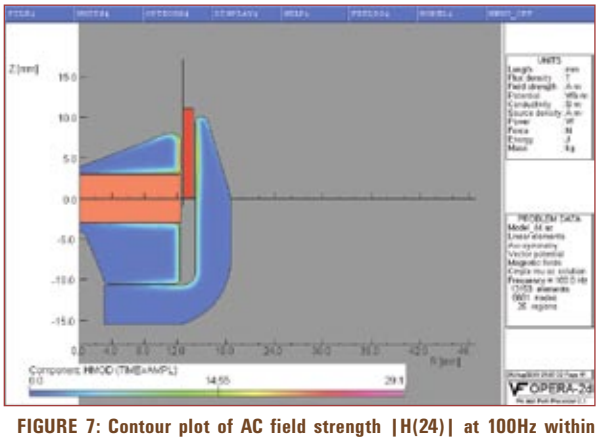

FIGURE 7: Contour plot of AC field strength |H(24)| at 100Hz within the steel only.

AC magnetic fields.

THE DC PROBLEM

I will begin with the DC problem. This is straightforward. The nonlinear DC problem can be defined by the nonlinear force factor, B*l*(*x*), equation 3.

$$\frac{F}{i}(x) = Bl(x)\left(\frac{N}{A}\right) \text{or} (Tm) \qquad (3)$$

F(*x*) (N) is the force. This force and thus the force factor vary with the voice coil position, *x* (***Fig. 3***). B is the DC flux density, where the DC flux density times the cross sectional area *S* (m^2) is the DC flux, ϕ (Wb), equation 4.

$$B \bullet S = \phi \qquad (4)$$

Figure 4 contains a contour plot of the solution for the magnitude of the DC flux density, |B| (T or Wb/m^2).

Figure 3 illustrates the command file simulation of the DC force factor, B*l*(*x*) and β(*x*),

$$Bl(\pm Xmax) = 0.82Bl(0) \qquad (5)$$

The DC command file implements equation 6; *N* is the number of turns of wire on the voice coil bobbin.

$$Bl(x) = \frac{Nd\phi(x)}{dx} = \frac{N\left[\phi(x + dx/2) - \phi(x - dx/2)\right]}{dx} \qquad (6)$$

The derivative is a moving difference in flux with respect to the voice coil wind height divided by the wind height!

β is the figure of merit for motor force regardless of the nominal voice coil impedance, equation 7.

$$\beta = \frac{(Bl)^2}{Re} = \frac{B^2(N2\pi r_{VC})^2 S_W}{N2\pi r_{VC}\sigma_W} = \frac{B^2}{\sigma_W} Vol_W\left(\frac{N^2}{W}\right) \qquad (7)$$

where σ_W (1/Ωm) is the conductivity of the voice coil wire and r_{VC} (m) is the radius of the voice coil and S_W (m^2) is the cross-section of the voice coil wire. Then for a given voice coil wire material, copper or aluminum, β depends only on the square of flux density and the volume of conductor, Vol_W (m^3) in the magnetic gap! Remember that β(*x*) is a DC quantity.

PERMEABILITY

Dynamically, current affects the permeability of the steel. This is what I call dynamic permeability, μ(*i*) (H/m). To explain the dynamic permeability I must first define the DC permeability μ in equation 8.

$$\mu = \frac{dB}{dH}\left(\frac{Tm}{A}\right) \qquad (8)$$

This is the slope of the material BH Curve. This is linear for air and for the magnet up to reasonable temperatures, but for steel the BH Curve is nonlinear (***Fig. 5***). A common way to represent the permeability is relative to the permeability of air, μ_0. Air is the poorest conductor of magnetic flux known. There are no known insulators of magnetic flux. See ***Fig. 4*** for the contour plot of the relative DC permeability.

$\mu_{rel} = \frac{\mu}{\mu_0}$ (unit-less) where $\mu_0 = 4\pi 10^{-7}$, the permeability of air, is a small constant. (9)

The AC problem is restarted from the DC permeability. There is an AC magnetic field with AC flux density, *B(i)* and AC magnetic field strength, *H(i)*, thus the dynamic permeability shown in equation 10 and ***Fig. 5***.

$$\mu(i) = \frac{B \pm B(i)}{H \pm H(i)} \text{ peak-to-peak} \qquad (10)$$

Figure 3 illustrates the dynamic permeability phenomenon with regard to a typical nonlinear BH Curve of steel.

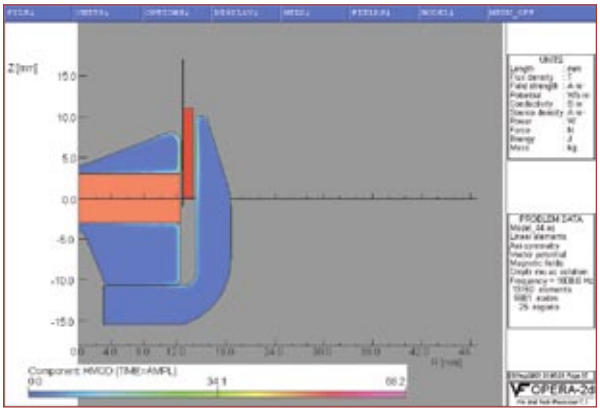

FIGURE 8: Contour plot of AC field strength |H(24)| at 1.0kHz within the steel only.

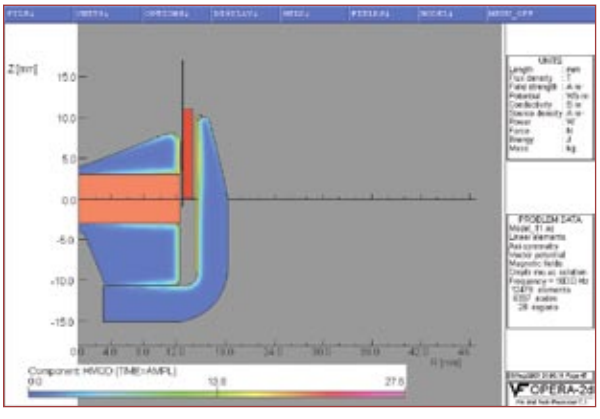

FIGURE 9: Contour plot of AC field strength |H(24)| at 100Hz with shorting ring.

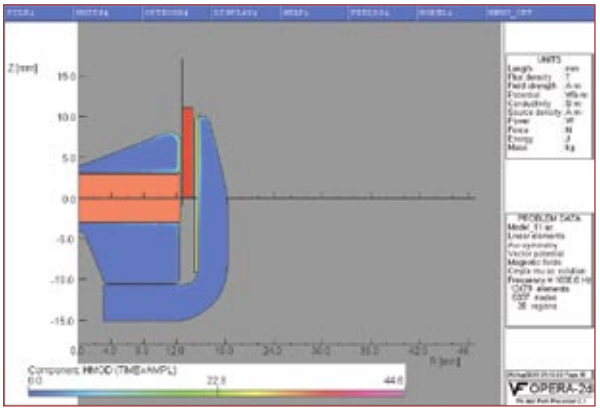

FIGURE 10: Contour plot of AC field strength |H(24)| at 1.0kHz with shorting ring.

Figure 6 illustrates the DC field strength |H| (A/m) within the steel. While ***Fig. 7*** shows the AC field strength |*H*| at 100Hz, ***Fig. 8*** shows |*H*| at 1.0kHz. ***Figures 9*** and ***10*** illustrate the AC field strength H in the steel alone at 100 and 1000Hz, respectively, but with a shorting ring. You can also observe the skin effect in ***Figs. 9*** and ***10***.

It is also an AC *H(i)* (***Figs. 12-15***) that combines with the DC field strength within the magnet (***Fig. 11***), but the permeability of the magnet is μ_0 (***Fig. 4***). There is also no skin effect and the eddy current is small; σ is low but not zero like air. The flux is coming from the current in the steel. The magnet almost behaves like a large air gap with regard to the AC problem.

The BH Curve of the "N48H" magnet is linear at room temperature but becomes nonlinear as temperature is increased (***Fig. 16***). The operating point moves about the load line by ±*H(i)* as it does with the steel (***Fig. 5***). So by reducing eddy current within the steel, the shorting ring reduces the |H(i)| within the magnet, too.

In next month's issue, Part 2 will continue this look at inductance effects in transducer design. ***VC***

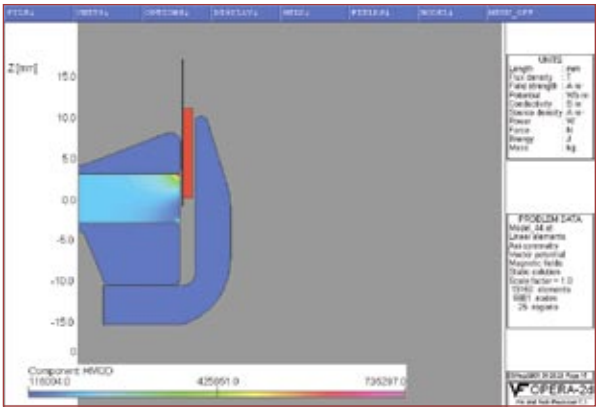

FIGURE 11: Contour plot of the DC field strength |H| within the magnet only.

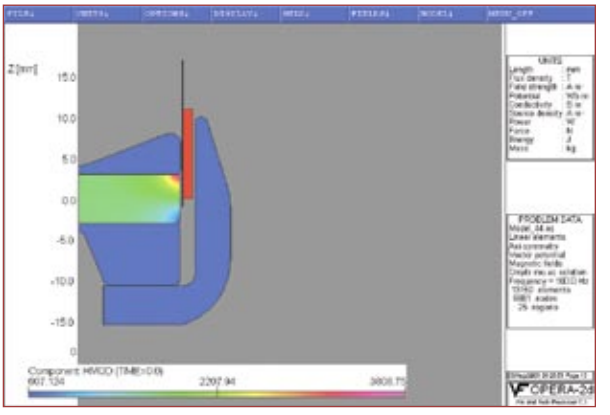

FIGURE 12: Contour plot of |H(24)| at 100Hz within the magnet only.

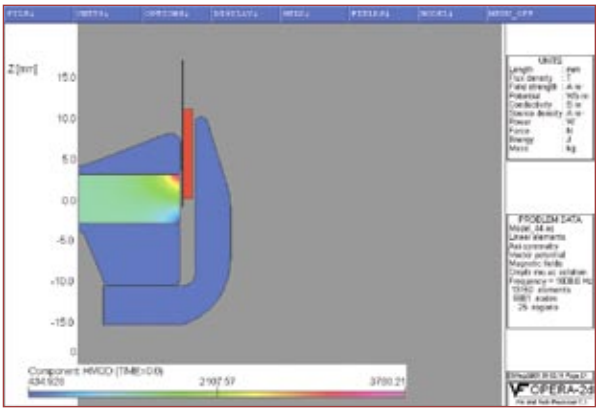

FIGURE 13: Contour plot of |H(24)| at 1.0kHz within the magnet only.

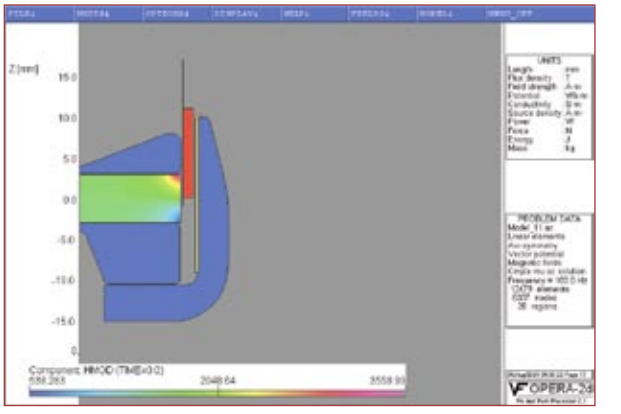

FIGURE 14: Contour plot of |H(24)| at 100Hz with shorting ring within the magnet only.

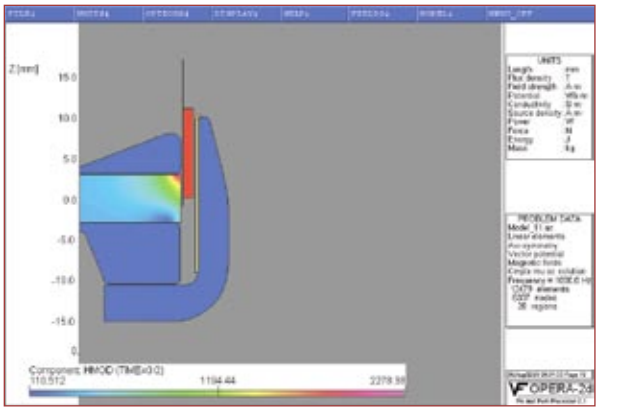

FIGURE 15: Contour plot of |H(24)| at 1.0kHz with shorting ring within the magnet only.

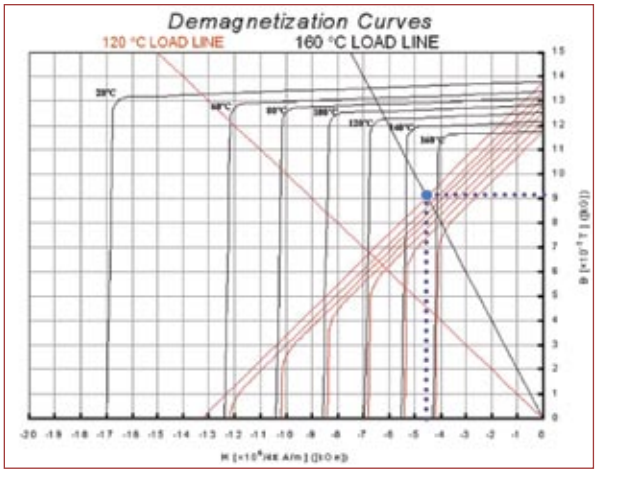

FIGURE 16: Temperature dependent N48H BH curves.

VOICE COIL
THE PERIODICAL FOR THE LOUDSPEAKER INDUSTRY

Article prepared for www.audioXpress.com

Inductance et al.—A Closer Look at AC, Part 2

By Steve Mowry

THE AC PROBLEM

I will pick up this discussion of inductance factors within the motor assembly with perhaps the most dreaded of all equations, Maxwell's AC electromagnetic vector equation in integral form!

$$\int E \cdot \mathrm{dl} = -\int\int \mathrm{T}m \cdot \mathrm{dS} - \frac{\mathrm{d}}{\mathrm{dt}} \int\int B \cdot \mathrm{dS}(\mathrm{V}) \qquad (11)$$

All this means is that the electric field E (V/m) is related to the magnetic charge density, Tm (V/m^2) and the time varying AC flux density, (Wb/m^{2}s) or (T/s). Fortunately, for this case you can simplify the equation, but as in the DC problem these are nonlinear electromagnetic quantities that depend on voice coil position, x, and current, i.

$$-E(\mathrm{x}) = \frac{\mathrm{J}}{\sigma}(\mathrm{x}) + \frac{\mathrm{d}}{\mathrm{dt}} \frac{\varphi}{2\pi \mathrm{r}}(\mathrm{x,i}) \qquad (12)$$

where J (A/m^2) is the "AC eddy current density"; r is the radius, (m); σ is the electrical conductivity (1/Ωm), and $\frac{\mathrm{d}\varphi}{\mathrm{dt}}$ (Wb/s) is the time varying magnetic flux.

What this means is that where there is an AC electric field, there is current and a time varying magnetic field. Remember that all those loudspeaker magnets are DC permanent magnets. The DC magnetic field does not change with time.

In the copper or aluminum shorting ring(s) where $\mu = \mu_0$ (Fig. 2 in Part 1), the permeability of air (H/m), the induction is small and is assumed zero. While in the magnet, the conductivity, σ, is quite small and $\mu = \mu_0$, thus the AC induction is assumed zero and the resistivity, $1/\sigma$, is large. Thus the magnet is treated as air with regard to the AC model segment. Remember that the AC magnetic fields are the results of the AC current i in the voice coil.

Then the AC voltage in the voice coil produces an AC electric field and thus an AC eddy current density, J, and time varying flux result within the motor assembly. Figures 9-14 in Part 1 illustrate these quantities and show that they change with voice coil position and the skin depth changes with frequency. This is illustrated in the left-hand segment of the model in Fig. 1.

The AC problem is inherently separate from the DC problem in that the DC flux and the DC flux density do not change with time:

$$\frac{\mathrm{dB}}{\mathrm{dt}} = 0 \text{ and } \frac{\mathrm{d}\phi}{\mathrm{dt}} = 0 \qquad (13)$$

The AC magnetic field does change with time:

$$\frac{\mathrm{d}B}{\mathrm{dt}} \neq 0 \text{ and } \frac{\mathrm{d}\varphi}{\mathrm{dt}} \neq 0 \qquad (14)$$

$\frac{\mathrm{d}}{\mathrm{dt}}$ is the notation for the rate of change of a quantity with respect to time, (1/s).

The *VECTOR FIELDS* PC OPERA 2d finite element analysis software restarts the AC steady-state harmonic analysis from the DC permeability. Subsequently, the solution to the DC and AC problems can be displayed separately. Look at the steady-state solutions to the AC problem to further explain the dynamic permeability and other AC phenomena.

Figures 17-22 contain plots of the eddy current density, J(x) at x = Xmax, 0 and – Xmax at 100 and 1000Hz. It is clear that the eddy current density changes with voice coil position, x.

Figures 23-28 contain contours of the AC flux lines, $\varphi(x)$, that illustrate that the AC magnetic field changes with voice coil position and frequency as the skin depth, δ, changes. The peak $|B|$ is also plotted on the color scale but the flux lines hide the skinned AC flux density.

The inductance, Le, is simply the total AC flux linkage, $N\varphi$ (Wb) with respect to the voice coil divided by the AC current, i (A) (equation 15), where N is the number of turns

of voice coil wire.

$$Le = \frac{N\varphi}{i}(H) \qquad (15)$$

Inductance and the AC force factor are related by the change in flux linkage with voice coil position divided by the voice coil wind height (equation 16). This is displayed in ***Fig. 42***.

$$\frac{dLe(x)i}{dx} = \frac{Nd\varphi(x)}{dx} = \frac{N\left[\varphi(x+dx/2)-\varphi(x-dx/2)\right]}{dx} = Bl(x) \qquad (16)$$

The command used to simulate inductance as illustrated in ***Fig. 41*** is shown in equation 17.

$$Le(x) = N\int_{dx}\frac{\varphi(x)}{i} = \frac{N\left[\varphi(x+dx/2)+\varphi(x-dx/2)\right]}{2i} \qquad (17)$$

The integration is just a moving average of the AC flux but with respect to the voice coil height, *dx*. However, equations 15 and 16 should be displaced and applied piecewise, three pieces minimum, to the finite element models for the most accurate simulation.

Just as the DC flux density linking to current in the voice coil results in a force, the AC flux density also links to the current in the voice coil (***Fig. 42***), which results in an AC reluctance force. For a sinusoidal signal, the reluctance force, shown in equation 18, also depends on the skin depth.

$$Fm(\delta,x,i) = \frac{Bl(\delta,x,i)i}{2}(N) \qquad (18)$$

With the shorting ring, the eddy current density within the steel is decreased and copper does not skin at audio frequencies. As frequency increases the shorting ring is more effective. The ferromagnetic material is skinning and the shorting ring is essentially shorting the inductance (Fig. 1).

EDDY CURRENT LOSS

The resistance that the voice coil sees as a result of the AC eddy current within the silver, copper, or aluminum-shorting ring is shown in relationship 19.

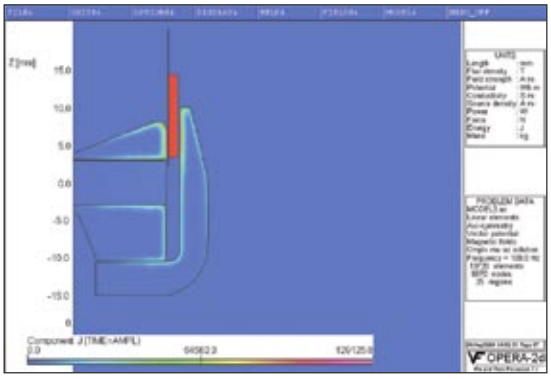

FIGURE 17: Contour plot of eddy current density $|J|$ at 100Hz, *x* = Xmax, *i* = 24A.

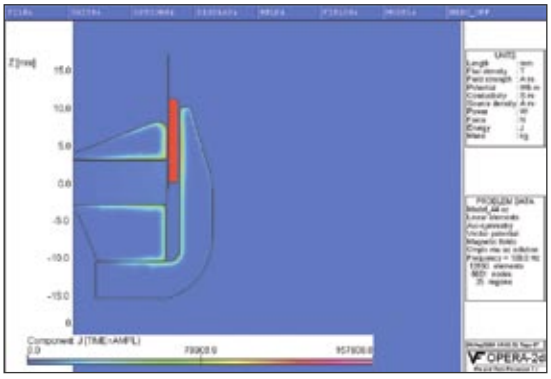

FIGURE 18: Contour plot of eddy current density $|J|$ at 100Hz, *x* = 0, *i* = 24A.

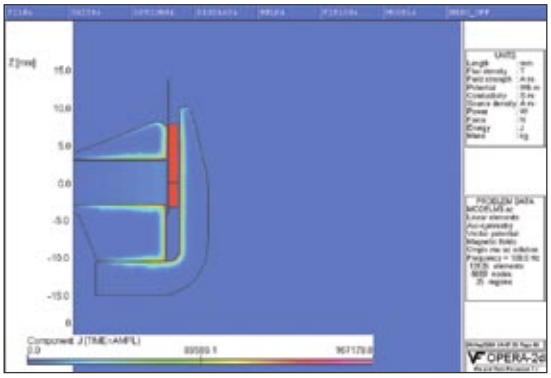

FIGURE 19: Contour plot of eddy current density $|J|$ at 100Hz, *x* = -Xmax, *i* = 24A.

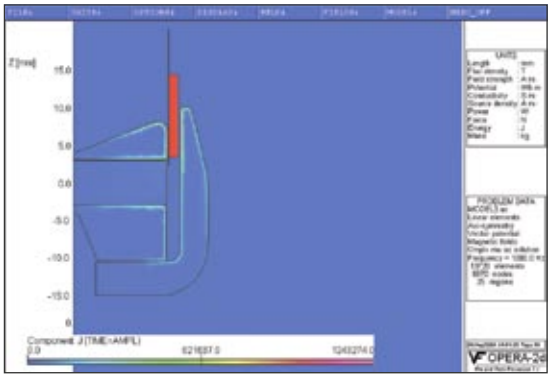

FIGURE 20: Contour plot of eddy current density $|J|$ at 1.0kHz, *x* = Xmax, *i* = 24A.

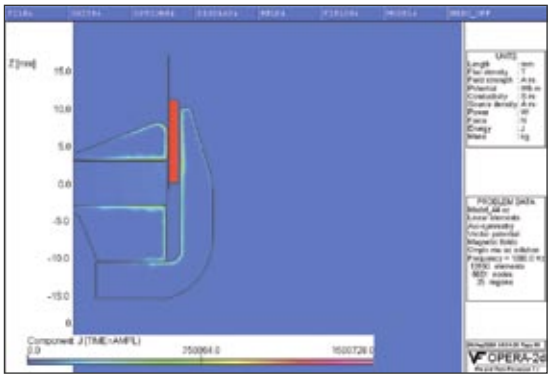

FIGURE 21: Contour plot of eddy current density $|J|$ at 1.0kHz, *x* = 0, *i* = 24A.

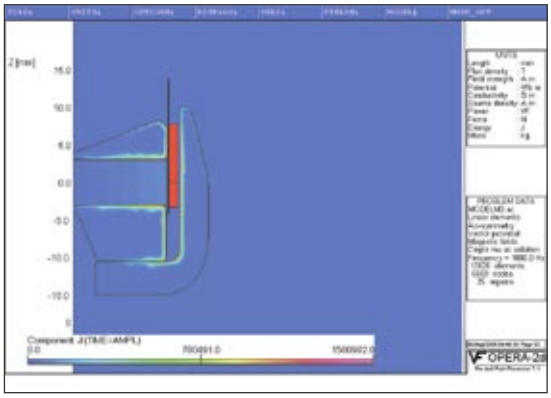

FIGURE 22: Contour plot of eddy current density $|J|$ at 1.0kHz, *x* = -Xmax, *i* = 24A.

$$R_{SR}\alpha\frac{2\pi r}{\sigma_{SR}\cdot S_{SR}}(\Omega) \qquad (19)$$

Where typically the radius of the shorting ring/shorted turn is approximately equal to the radius of the voice coil; the high conductivity of the shorting ring does, in effect, short the eddy current especially as frequency is increased; and the steel skin depth becomes small. To further improve the linearization due to the shorting ring at low frequencies, increase the cross-section, S_{SR}. A real challenge with shorting ring design can be strategic placement. Real estate within the magnetic gap is critical, and typically the thickness is limited to 0.30mm (0.012″). However, there are alternatives to placing the ring in the gap and you can select many other combinations of geometry and materials.

Figures 29-31 and ***Figs. 35-37*** illustrate the eddy current density, J_{SR}, within the shorting at 100 and 1000Hz, respectively. You can observe that the eddy current density changes somewhat with voice coil position, *x*. The current density in the shorting ring increases at 1000Hz; however, the current density in the steel decreases!

The permeability of the shorting ring is μ_0, the permeability of air. I ignored any frequency or current dependent skin effect. The resistance the voice coil sees due to eddy current losses within the shorting ring goes as the ratio of the length of the ring, the circumference to the cross-section times the conductivity of the shorting ring. Oxygen-free copper and aluminum are the most common materials for these rings; however, you can also use silver. The conductivity of these materials is high, while silver is the highest of all.

The resistance the voice coil sees as a result of the AC eddy current within the ferromagnetic material depends on the skin depth and is shown in relationship 20.

$$R_{FM}(\delta)\alpha\frac{2\pi r}{\sigma_{FM}\cdot S_{FM}}\sim\frac{2\pi r}{\sigma_{FM}\cdot(x_o+\delta)}(\Omega) \qquad (20)$$

As the skin depth δ is reduced, the resistance will increase. $z_o+\delta$ and $r_o+\delta$ are the vertical and horizontal skin sections, respectively, in the contours of AC eddy current density illustrated in ***Figs. 17-22***. The cross-section, S_{FM}, is

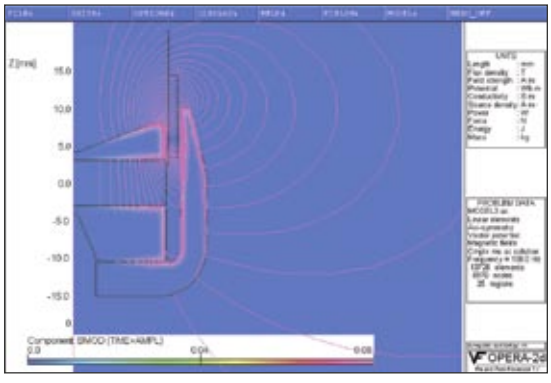

FIGURE 23: Contour plot of AC flux lines, φ at 100Hz, *x* = Xmax, *i* = 24A.

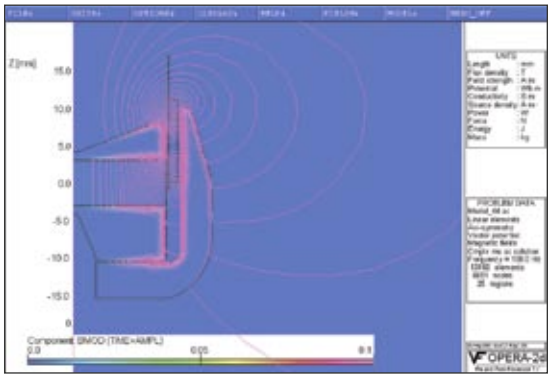

FIGURE 24: Contour plot of AC flux lines, φ at 100Hz, *x* = 0, *i* = 24A.

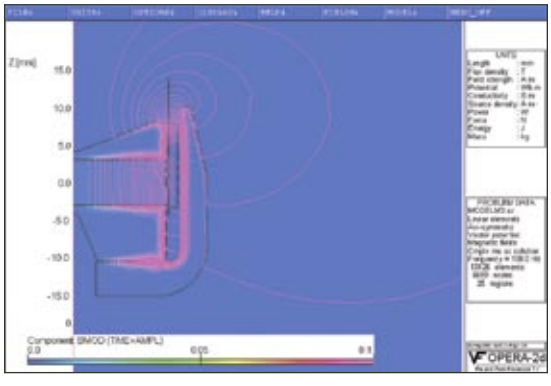

FIGURE 25: Contour plot of AC flux lines, φ at 100Hz, *x* = -Xmax, *i* = 24A.

FIGURE 26: Contour plot of AC flux lines, φ at 1.0kHz, *x* = Xmax, *i* = 24A.

FIGURE 27: Contour plot of AC flux lines, φ at 1.0kHz, *x* = 0, *i* = 24A.

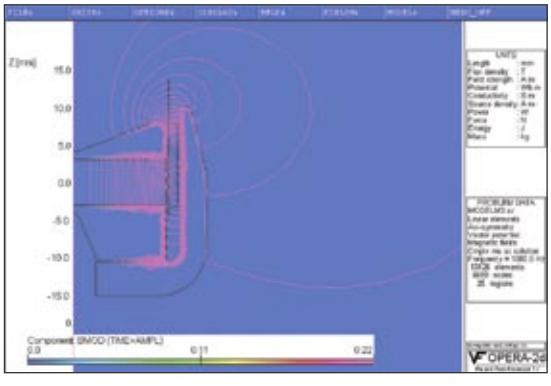

FIGURE 28: Contour plot of AC flux lines, φ at 1.0kHz, *x* = -Xmax, *i* = 24A.

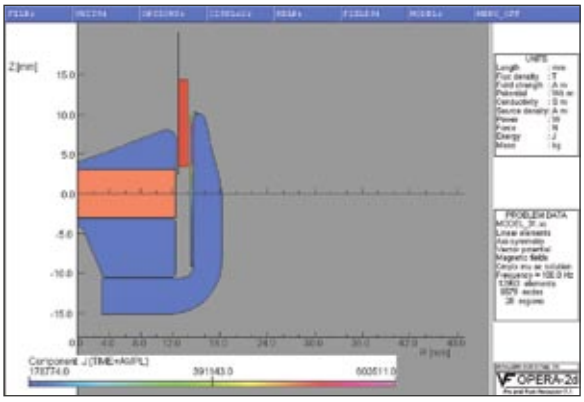

FIGURE 29: Contour plot of $|J_{SR}|$ within shorting ring only at 100Hz, x = Xmax, i = 24A.

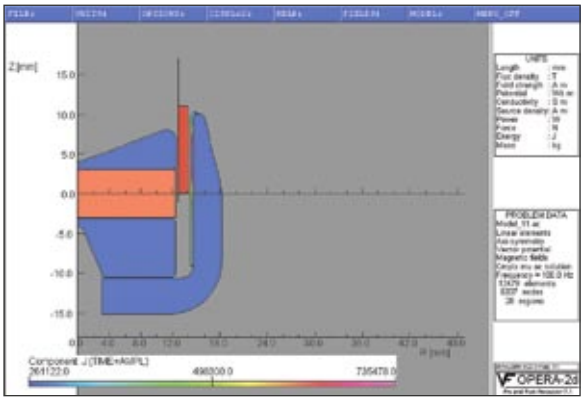

FIGURE 30: Contour plot of $|J_{SR}|$ within shorting ring only at 100Hz, x = 0, i = 24A.

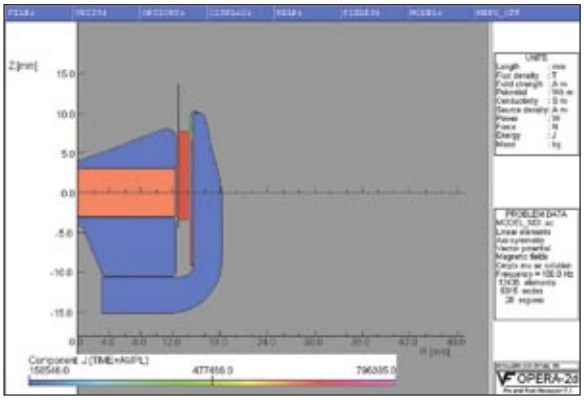

FIGURE 31: Contour plot of $|J_{SR}|$ within shorting ring only at 100Hz, x = -Xmax, i = 24A.

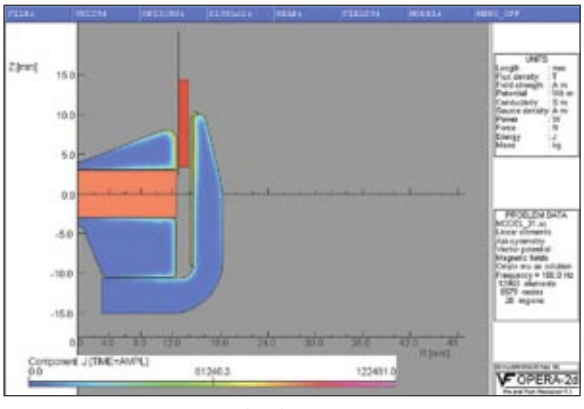

FIGURE 32: Contour plot of $|J_{FM}|$ within the steel only at 100Hz, x = Xmax, i = 24A.

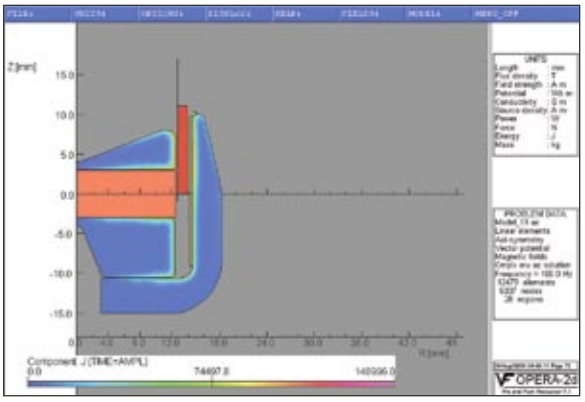

FIGURE 33: Contour plot of $|J_{FM}|$ within the steel only at 100Hz, x = 0, i = 24A.

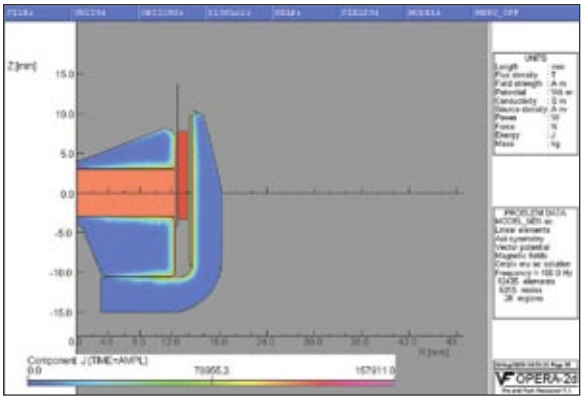

FIGURE 34: Contour plot of $|J_{FM}|$ within the steel only at 100Hz, x = -Xmax, i = 24A.

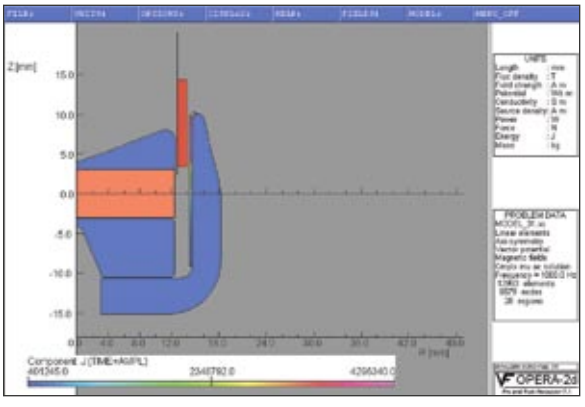

FIGURE 35: Contour plot of $|J_{SR}|$ within shorting ring only at 1.0kHz, x = Xmax, i = 24A.

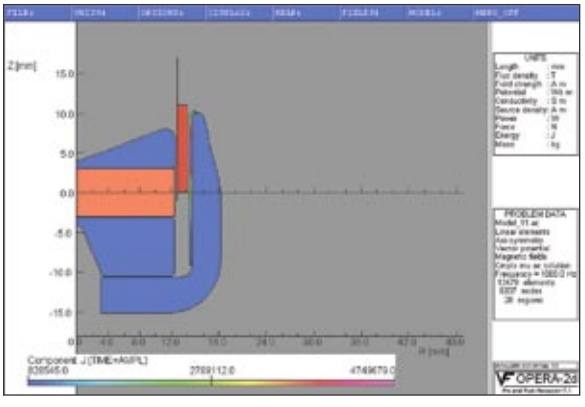

FIGURE 36: Contour plot of $|J_{SR}|$ within shorting ring only at 1.0kHz, x = 0, i = 24A.

effectively reduced. The eddy current losses then go inversely as the conductivity, σ_{FM}, and the skinned cross-section. The function of the shorting ring is to reduce the effective resistance and inductance, thus the eddy current within the steel due to the current division. This is clearly indicated by the model illustrated in Fig. 1, and you can see it in ***Figs. 32-34*** and ***Figs. 38-40***. These quantities are material dominated and are best controlled with a shorting ring(s). The objective is to short the R_{FM} and the Le with the high conductivity (low resistance copper or aluminum). This typically reduces loss and inductance.

CONCLUSION

I have presented a detailed discussion of the AC electromagnetic phenomenon and developed a model that relates to materials, geometry, and the voice coil within the motor assembly. When you use this model with finite element analysis and command files, a powerful simulation and design tool is realized. The modeling goes quickly and typically a complete motor design can be completed in one to two weeks. Motor nonlinearities are identified in such a way as to assist the transducer designer in quickly obtaining meaningful motor assembly information.

Within the DC problem the major nonlinear mechanism is the voice coil displacement $x(t)$ resulting from the AC current, $i(t)$. Within the AC problem the voice coil displacement, $x(t)$, is still a nonlinear mechanism; however, the magnetic field density is also changing with time, $B(x,t)$. Then it follows that the AC eddy current density is also changing with voice coil position and time, $J(x,t)$, because the eddy current is the major source of the AC flux, $\varphi(x,t)$. If that wasn't enough, I have shown that these AC quantities also change with current, i, $\varphi(x,i,t)$ and $B(x,i,t)$ due to changes in the dynamic permeability, $\mu(i,t)$. Finally, there is the AC skin effect in steel that adds losses and changes in eddy current density, $J(\delta,x,t)$ and changes in flux, $\varphi(\delta, x,i,t)$, where $\delta \alpha \frac{1}{\sqrt{f}}$ in the limit.

These are the nonlinear mechanisms within the motor assembly. The AC mechanisms are essentially all related to inductance and inductance modulation. If this is all starting to seem chaotic, it's not surprising. Nonlinearity and distortion are chaos. ***VC***

Download my BH Curve text files at
www.s-m-audio.com/SM_Audio_BH_Curves.zip.

Download my material property table including conductivity, σ, for common motor assembly materials at
www.s-m-audio.com/ENGINEERING_MATERIAL_PROPERTIES.zip

Download my Voice Coil Worksheet at
www.s-m-audio.com/SM_AUDIO_VOICE_COIL_WORKSHEET.zip

A special thanks to the technical staff at Advanced Sound Technology Sdn. Bhd. (MSC) for their support. Happy inductance modeling.

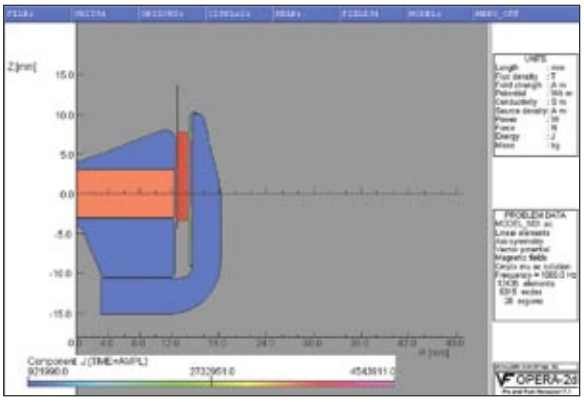

FIGURE 37: Contour plot of $|J_{SR}|$ within shorting ring only at 1.0kHz, x = -Xmax, i = 24A.

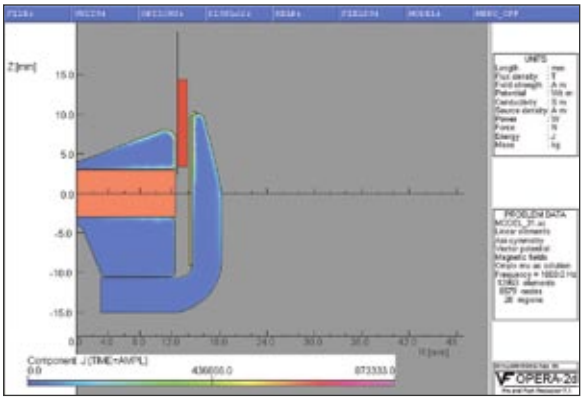

FIGURE 38: Contour plot of $|J_{FM}|$ within the steel at 1.0kHz, x = Xmax, i = 24A.

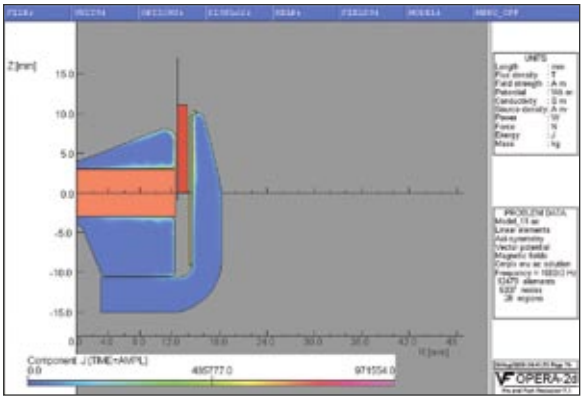

FIGURE 39: Contour plot of $|J_{FM}|$ within the steel only at 1.0kHz, x = 0, i = 24A.

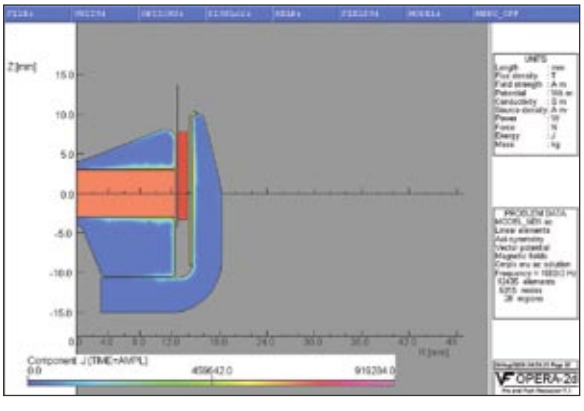

FIGURE 40: Contour plot of $|J_{FM}|$ within the steel only at 1.0kHz, x = -Xmax, i = 24A.

Steve Mowry, president of SM Audio Engineering, has a BS, Business Administration, from Bryant College, and a BS and MS, Electrical Engineering, from URI with highest distinction. Steve has worked in R&D at BOSE, TC Sounds, EASTTECH, and P.Audio. Steve is currently an independent consultant/lecturer in project management/transducer and system design. His website is www.s-m-audio.com.

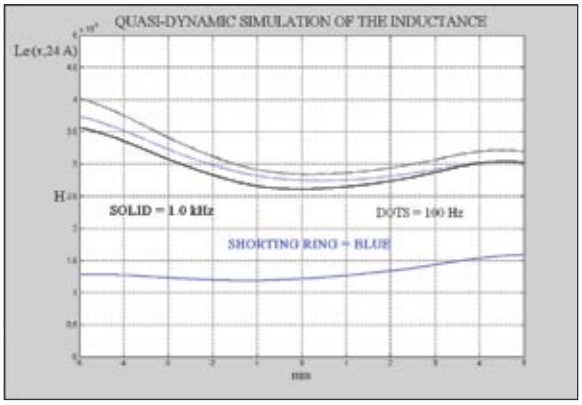

FIGURE 41: Quasi-dynamic simulation of inductance, |Le(*x*, 24A)| at 24A at 100Hz and 1.0kHz with and without shorting ring.

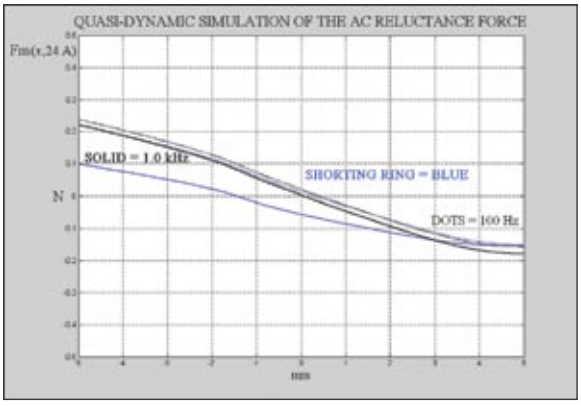

FIGURE 42: Quasi-dynamic simulation of the AC reluctant force, Fm(*x*, 24A) at 24A at 100Hz and 1.0kHz with and without shorting ring.